ACS Chemical Neuroscience
Cite This: ACS Chem. Neurosci. 2019, 10, 1603−1614
Research Article
pubs.acs.org/chemneuro

Biodegradable Nanoparticles Containing Mechanism Based Peptide Inhibitors Reduce Polyglutamine Aggregation in Cell Models and Alleviate Motor Symptoms in a *Drosophila* Model of Huntington's Disease

Abhayraj S. Joshi, Virender Singh, Avinash Gahane, and Ashwani Kumar Thakur*

Department of Biological Sciences & Bioengineering, Indian Institute of Technology Kanpur (IIT Kanpur), Kanpur, Uttar Pradesh, India 208016

Supporting Information

Downloaded via UNIV OF SOUTH DAKOTA on November 6, 2019 at 22:42:15 (UTC).
See https://pubs.acs.org/sharingguidelines for options on how to legitimately share published articles.

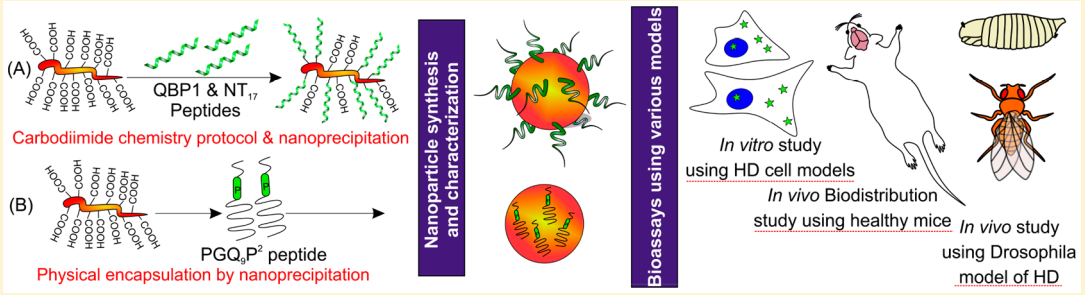

ABSTRACT: Detailed study of the molecular mechanism behind the pathogenesis of Huntington's disease (HD) suggests that polyglutamine aggregation is one of the fundamental reasons for HD. Despite the discovery of many potential molecules, HD therapy is still limited to symptomatic relief. Among these molecules, few mechanism based peptide inhibitors of polyglutamine aggregation (QBP1, NT_{17} and PGQ_9P^2) have shown promising activity; however, poor blood-brain barrier (BBB) penetration, low bioavailability, and low half-life may hinder their therapeutic potential. Hence, to deliver them to the brain for assessing their efficacy, we have designed and synthesized peptide loaded poly-D,L-lactide-*co*-glycolide (PLGA) nanoparticles of less than 200 nm in size by carbodiimide chemistry and nanoprecipitation protocols. For brain delivery, PLGA nanoparticles were coated with polysorbate 80 which aids receptor mediated internalization. Using the in vitro BBB model of Madin-Darby canine kidney cells and healthy mice, the translocation of polysorbate 80 coated fluorescent nanoparticles was confirmed. Moreover, QBP1, NT_{17}, and PGQ_9P^2 loaded PLGA nanoparticles showed dose dependent inhibition of polyglutamine aggregation in cell models of HD (Neuro 2A and PC12 cells) and improved motor performance in *Drosophila* model of HD. Additionally, no toxicity in cells and animals confirmed biocompatibility of the nanoparticulate formulations. Based on this work, future studies can be designed in higher animal models to test peptide loaded nanoparticles in HD and other polyglutamine expansion related diseases.

KEYWORDS: *Huntington's disease, polyglutamine aggregation, peptide inhibitors, blood-brain barrier, carbodiimide chemistry, PLGA nanoparticles*

INTRODUCTION

Huntington's disease is a hereditary neurodegenerative disease which occurs due to CAG repeat expansion resulting from mutation in the *IT15* gene. It results in the expression of mutant huntingtin protein (mHtt) with an expanded polyglutamine tract (PolyQ, Q_n > 40).[1,2] Proteolytic cleavage of the mHtt leads to the formation of N-terminal fragments with pathogenic PolyQ which undergo a complex aggregation cascade to form β-sheet rich amyloidic aggregates in striatal and cortical neurons.[3−5] The role of these aggregates and intermediate species in the etiology of HD remains a mystery; however, many reports suggest that these aggregates and aggregation intermediates might be the basis of neurodegeneration.[6] The polyglutamine aggregation and increased burden of aggregates lead to the downstream abnormalities in transcription, translation, mitochondrial function, autophagy, synthesis, and transport of neurotropic factors which culminate into the neuronal cell death. Thus, HD patients suffer from behavioral, cognitive, and motor symptoms.[1]

Despite remarkable efforts toward drug development in HD, to date, only two drugs have been approved by the United States Food and Drug Administration (FDA) which provide only symptomatic treatment.[7] However, understanding of the molecular mechanism of HD neuropathology has identified

Received: October 10, 2018
Accepted: November 19, 2018
Published: November 19, 2018

ACS Publications © 2018 American Chemical Society

DOI: 10.1021/acschemneuro.8b00545
ACS Chem. Neurosci. 2019, 10, 1603−1614

Table 1. Amino Acid Sequence and Nomenclature of Peptide Inhibitors of Polyglutamine Aggregation Used in the Study

name[a]	amino acid sequence
PGQ_9P^2	KKQQQQQQQQQPGQQQQPQQQQPGQQQQQQQQQPGQQQQQQQQQKK
QBP1	SNWKWWPGIFD
NT_{17}	MATLEKLMKAFESLKSF

[a]Detailed information about nomenclature of peptides can be found in the Supporting Information.

potential therapeutic targets which include the genetic mutation, aggregation of mHtt, and downstream cellular defects. Against these targets, several oligonucleotides, peptides, and small synthetic and natural molecules have been developed.[1,8−10] Among them, some peptide inhibitors (NT_{17}, PGQ_9P^2, $PGQ_9P^{2,3}$, $PGQ_9P^{1,2,3}$, P42, and QBP1-QBP6) have shown great inhibitory potential against mHtt aggregation;[10−14] whereas few other peptides such as IC10,[15] CAM peptide,[16] and Extendin-4[17] have shown action against the cellular defects of HD. Currently, their therapeutic potential remains underexplored because, except for Extendin-4, no report confirms penetration of other peptides across the blood-brain barrier (BBB). Additionally, they may undergo degradation in vivo by several proteolytic enzymes, resulting in poor specificity, low bioavailability, and limited efficacy. These challenges imply a growing necessity of a drug delivery platform for taking these peptide inhibitors to the brain for inhibition of aggregation.

The nanoparticulate delivery system has applications in the fields of biology and medicine because it offers improved target specificity, improved shelf life of a drug, increased bioavailability of a drug, and reduction in side effects.[18] To our knowledge, no report is available that shows successful delivery and efficacy of these peptide inhibitors in vitro and in vivo with an exception of P42 peptide.[14,19] This gap in research poses a problem in testing these molecules in the preclinical phase before their translation to effective drugs through clinical trials.

Previously, we have shown successful encapsulation of one polyglutamine aggregation inhibitor, PGQ_9P^2 peptide (Table 1), in biodegradable poly-D,L-lactide-*co*-glycolide (PLGA) nanoparticles, its release from nanoparticles, and inhibition of elongation of an aggregation prone peptide in vitro.[20] In this article, we demonstrate the conjugation of two other inhibitors of polyglutamine aggregation (QBP1 and NT_{17}, Table 1) as well as dyes to PLGA polymer using carbodiimide chemistry to prepare peptide loaded and dye loaded polymer. Using a previously established nanoprecipitation protocol,[20] the peptide loaded and dye loaded PLGA nanoparticles were prepared. For brain targeting, we used a well-known strategy of polysorbate 80 coating which leads to preferential adsorption of apolipoprotein E (ApoE) and transcytosis via low density lipoprotein (LDL) receptors.[21] Using an in vitro BBB model of Madin-Darby canine kidney (MDCK) cells, polysorbate 80 mediated transcytosis of fluorescent PLGA nanoparticles was confirmed. Biodistribution study in healthy mice corroborated with these results. Separately, the efficacy of peptide inhibitors against polyglutamine aggregation was analyzed in Neuro 2A and PC12 cell models of HD. Finally, in vivo efficacy of the peptide inhibitor loaded nanoparticles was evaluated with respect to the motor performance in the *Drosophila* model of HD at larval and adult stages. Collectively, our results show (i) successful delivery of fluorescent nanoparticles owing to polysorbate 80 coating across the MDCK monolayer and in healthy mouse brain and (ii) efficacy of peptides in cell models of HD and *Drosophila* model of HD.

RESULTS AND DISCUSSION

Synthesis of Peptide Loaded Nanoparticles (QBP1-NPs, NT_{17}-NPs, and PGQ_9P^2-NPs), Nanoprecipitation Yield, and Loading Efficiency. To synthesize PGQ_9P^2 peptide loaded nanoparticles, a conventional nanoprecipitation protocol was employed as per our previous report;[20] whereas QBP1 and NT_{17} peptides were first conjugated with carbodiimide chemistry and then nanoprecipitation was performed. Many reports have shown conjugation of peptides on the surface of preformed nanoparticles.[22,23] However, conjugating with polymer before nanoprecipitation (Figure 1, A and B) would lead to high QBP1 and NT_{17} loading per unit mass of polymer which would be low in other case because of limited availability of free carboxylic groups on PLGA

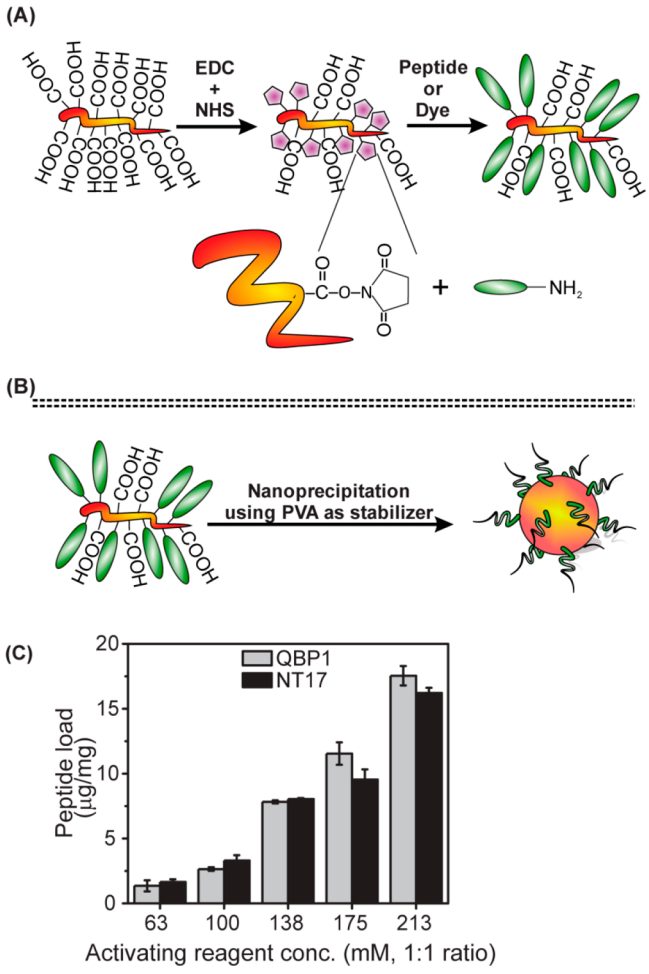

Figure 1. (A) Schematic for activation of carboxylic groups of PLGA polymer and subsequent attachment of peptide/dye to activated carboxylic groups. (B) Schematic for nanoprecipitation method to prepare nanoparticles from peptide/dye conjugated PLGA polymer. (C) Amount of QBP1 and NT_{17} peptides conjugated to PLGA polymer (μg/mg) determined by RP-HPLC method.

DOI: 10.1021/acschemneuro.8b00545
ACS Chem. Neurosci. 2019, 10, 1603−1614

nanoparticle surface.[22,24] Also, conjugating QBP1 and NT_{17} on the nanoparticle surface might make them vulnerable for degradation which would be minimal in our strategy as peptides are masked under PLGA chains.[22,24] Thus, conjugation was performed before nanoparticle synthesis. First, −COOH groups of the PLGA polymer were activated using 1-ethyl-3-(3-(dimethylamino)propyl) carbodiimide (EDC) and *N*-hydroxysuccinimide (NHS) (Figure 1A). PLGA activation and the carbodiimide reaction products (anhydride as dominant product) were confirmed with attenuated total reflectance Fourier transform infrared (ATR-FTIR) spectroscopy (Figures S1 and S2). Then, peptide conjugation was performed and confirmed using reversed phase-high performance liquid chromatography (RP-HPLC) (Figure 1C). Using peptide conjugated PLGA polymer and the nanoprecipitation protocol, QBP1-NPs and NT_{17}-NPs were synthesized (Figure 1B). No irregular precipitation/sedimentation of nanoparticles prepared from conjugated polymer during the nanoprecipitation method indicates that the conjugation protocol and/or peptides do not hinder the nanoparticle synthesis process. The conjugation efficiency was around 80−90% in all experiments for QBP1 and NT_{17}, whereas the nanoprecipitation yield for QBP1-NPs and NT_{17}-NPs was ∼75% which corroborates well with our previously published report.[20] This implies that the loading efficiency ranges from 2 to 18 μg/mg for QBP1-NPs and from 2 to 16 μg/mg for NT17-NPs for NT_{17}-NPs. On the other hand, PGQ_9P^2 peptide was physically encapsulated in PLGA chains with the conventional nanoprecipitation method as described previously.[20]

Dynamic Light Scattering (DLS) Analysis of Empty, Peptide Loaded, and Fluorescent Nanoparticles. DLS characterization of empty, peptide loaded and fluorescent PLGA nanoparticles showed size less than 200 nm (Table 2). Nanoparticles above 200 nm possess low in vivo half-life because of activation and degradation by reticuloendothelial system.[25] Also, for brain delivery, the desirable particle size is below 200 nm.[26] In the case of PGQ_9P^2-NPs, the size is significantly higher than that of ENPs (*t* test, *p*-value <0.05) because of physical entrapment of large peptide which validates our previous findings.[20] The size of NT_{17}-NPs is significantly different only in the highest NT_{17} peptide load from that of ENPs (*t* test, p-value <0.05); whereas QBP1-NPs showed significantly different size at all peptide loading levels (*t* test, *p*-value <0.05). It is possible that, a higher number of conjugated NT_{17} molecules leads to significantly different particle size unlike low and intermediate loading where particle size is statistically similar to that of ENPs. On the other hand, QBP1 assumes extended disordered structure leading to higher particle size at all loading levels as observed in FTIR results (Figure S3). Among the fluorescent nanoparticles, PLGA-Atto 590 NPs showed statistically same particle size as compared to ENPs; whereas, PLGA-Neutral red NPs showed higher particle size because of higher dye loading. PDI values for all nanoformulations remained below 0.1 suggesting uniform and narrow size distribution of the nanoparticles. Further, for ENPs, peptide loaded nanoparticles and PLGA-Atto 590 NPs, the zeta potential values were in the range of −20 to −30 mV and it corroborates well with our previous report.[20] However, PLGA-Neutral Red NPs showed significantly different zeta potential (−9 mV). This was observed probably because of conjugation of more dye molecules on the surface of PLGA nanoparticles.[27] Previously, using scanning electron microscopy (SEM), we have shown that PGQ_9P^2-NPs have nearly spherical shape.[20] SEM images of representative QBP1-NPs and NT_{17}-NPs also showed nearly spherical shape for all particles (Figure S4). Conjugation had no effect on surface morphology, suggesting the possibility of even masking of the surface by PVA chains which in turn indicates good stability of nanoparticles. In electron micrographs, few nanoparticles were present as fused particles which may be a drying artifact.[20] Overall DLS analysis of nanoparticles shows uniformly distributed nanoparticles with size below 200 nm, and negative zeta potentials which are desirable characteristics for a delivery system intended for brain targeting.[26] In separate experiments, QBP1 and NT_{17} peptide release from PLGA nanoparticles was also confirmed with RP-HPLC method[20] (Figure S5).

Table 2. DLS Characterization of Empty, Peptide Loaded, and Fluorescent PLGA Nanoparticles

nanoparticle batch	size (*d*, nm)[a]	PDI[b]	ZP (mV)[c]
ENPs	143 ± 10	0.043 ± 0.016	−27.5 ± 4.6
PGQ_9P^2-NPs	178 ± 8[d]	0.049 ± 0.021	−24.3 ± 6.6
NT_{17}-NPs (63 mM EDC-NHS+PLGA)[e]	158 ± 6	0.035 ± 0.006	−25.3 ± 4.9
QBP1-NPs (63 mM EDC-NHS+PLGA)[e]	164 ± 6[d]	0.038 ± 0.032	−25.3 ± 8.7
NT_{17}-NPs (100 mM EDC-NHS+PLGA)[e]	159 ± 2	0.031 ± 0.029	−27.3 ± 5.9
QBP1-NPs (100 mM EDC-NHS+PLGA)[e]	171 ± 6[d]	0.066 ± 0.026	−26.0 ± 6.9
NT_{17}-NPs (175 mM EDC-NHS+PLGA)[e]	174 ± 6[d]	0.065 ± 0.019	−23.3 ± 8.1
QBP1-NPs (175 mM EDC-NHS+PLGA)[e]	180 ± 8[d]	0.060 ± 0.021	−25.5 ± 3.8
PLGA-Atto 590 NPs	151 ± 9	0.089 ± 0.067	−22.8 ± 8.2
PLGA-Neutral red NPs	188 ± 8[d]	0.092 ± 0.040	−8.7 ± 2.3[d]

[a]Intensity weighted diameter, mean ± SD. [b]Polydispersity index, mean ± SD. [c]Zeta potential at pH 5−6, mean ± SD. [d]*t* test, *p*-value <0.05. [e]Information in parentheses represents concentration of EDC and NHS used for activation of PLGA and then the conjugation of peptide.

In Vitro and in Vivo Translocation of Fluorescent PLGA Nanoparticles (PLGA-Atto 590 NPs and PLGA-Neutral Red NPs). For targeting the brain, we used a polysorbate 80 coating strategy for the nanoparticles. Polysorbate 80 coating on the nanoparticles leads to preferential adsorption of ApoE which helps in internalization of nanoparticles through the LDL receptor mediated transcytosis process.[28] To confirm the translocation of fluorescent nanoparticles due to the polysorbate 80 coating, we first established an in vitro BBB model using MDCK cells. Its functional qualification was done in three ways: (i) measurement of transepithelial electrical resistance (TEER) value, (ii) analysis of permeability of standard solutes, and (iii) expression of tight junction protein (Figure S6). Using this model, the transcytosis experiments were performed (Figure 2A and B). In the first experiment, using transcytosis medium supplemented with 5% horse serum (HS), the transfer of uncoated and polysorbate 80 coated PLGA-Atto 590 nanoparticles was analyzed through the transwell inserts containing MDCK monolayer. The rate of transfer of polysorbate 80 coated nanoparticles (Figure 2A, red line) was significantly higher than that of uncoated nanoparticles (Figure 2A, green line) (*t* test, *p*-value < 0.05). Faster transfer rate of polysorbate 80 coated PLGA-Atto 590 NPs across in vitro BBB model as

DOI: 10.1021/acschemneuro.8b00545
ACS Chem. Neurosci. 2019, 10, 1603−1614

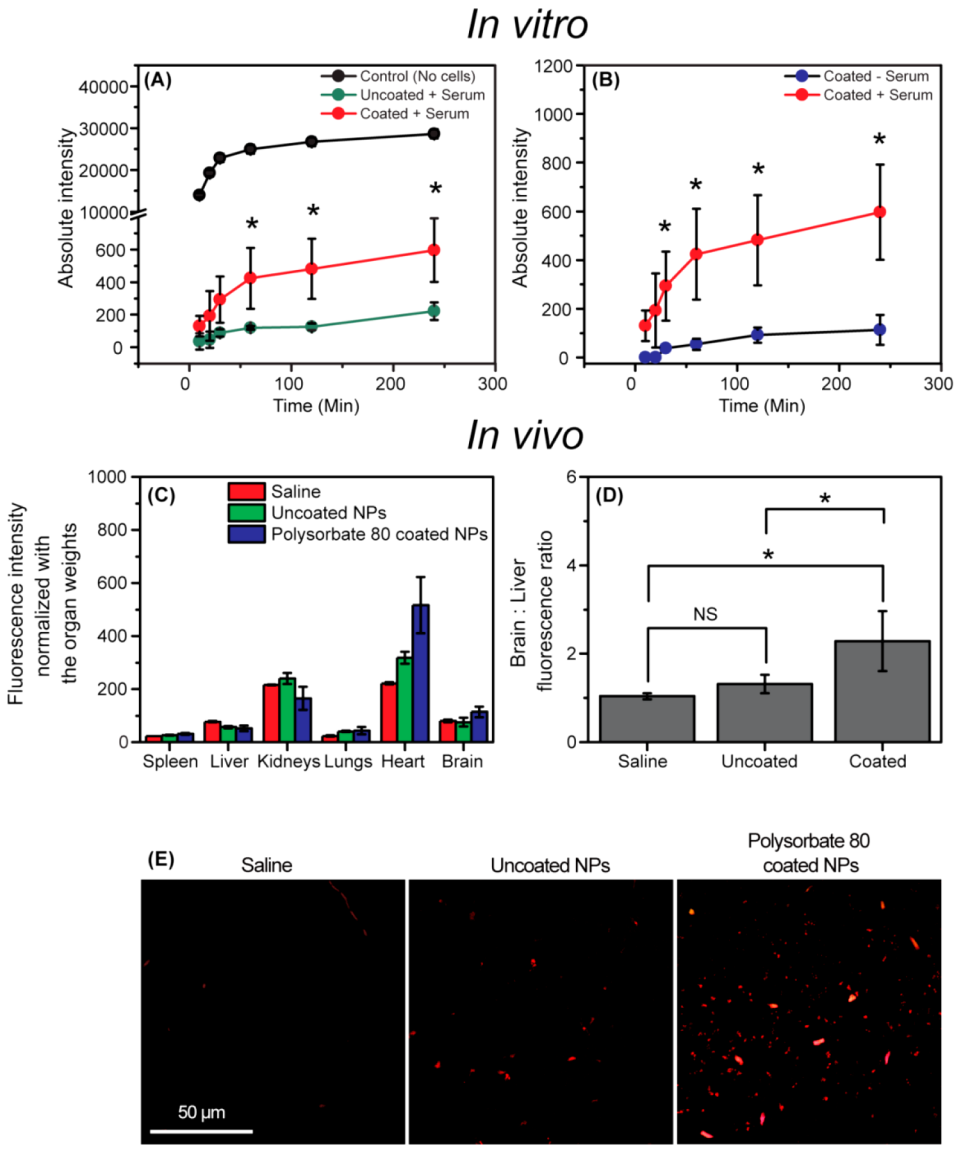

Figure 2. (A, B) Transcytosis of PLGA-Atto 590 NPs across MDCK cell monolayer in transwell inserts (in vitro). (C, D) Biodistribution of PLGA-Neutral red NPs in healthy mice (in vivo) before and after coating with polysorbate 80. (E) Representative confocal images of brain sections showing red fluorescence of neutral red after 2 h from intravenous injection. [Asterisk (*) in A, B, and D indicates significantly different observations, *t* test, *p*-value < 0.05. NS indicates no significant difference.]

compared to uncoated nanoparticles suggests that polysorbate 80 coat on the surface of nanoparticles has positive influence in the movement of nanoparticles from apical to basal chamber (Figure 2A). It is possible that gravitational force may play a role in the movement of nanoparticles across MDCK monolayers. To rule out this possibility and to confirm the role of ApoE, another experiment was performed in which transfer rate of polysorbate 80 coated PLGA-Atto 590 NPs was checked in presence and absence of horse serum (HS) (Figure 2B). The translocation of fluorescent nanoparticles was significantly higher in the presence of serum as compared to that in absence of serum. High accumulation in the presence of 5% HS and low accumulation in its absence strengthens the role of ApoE during transcytosis. We observed no resistance from transwell membrane for nanoparticles transfer (Figure 2A, black line). For in vivo biodistribution study, PLGA-Neutral red nanoparticles were used. PLGA-Neutral red polymer has advantage of large Stoke's shift (~140 nm) over PLGA-Atto 590 (~35 nm) which was used in our cell culture assays.[29] Also, previously it was reported that the average time for polysorbate 80 coated nanoparticles to reach the brain is ~1−3 h.[30] Hence, for biodistribution study in healthy mice, PLGA-Neutral red nanoparticles were injected in the tail vein and animals were sacrificed 2 h after injection. The spleen, liver, kidneys, lungs, heart, and brain were isolated, weighed, homogenized, and centrifuged. High fluorescence intensity was observed in heart, kidneys, and liver followed by brain (Figure 2C). At the 2 h time point from injection, the normalized intensity in the brain was significantly higher for polysorbate 80 coated nanoparticles as compared to uncoated nanoparticles (*t* test, *p*-value < 0.05). Further, the ratio of normalized fluorescence intensity in brain/liver is significantly higher (*t* test, *p*-value < 0.05) for polysorbate 80 coated nanoparticles as compared to uncoated nanoparticles (Figure 2D). These results are well corroborated with our in vitro results of transcytosis experiments. Also, the confocal images of

DOI: 10.1021/acschemneuro.8b00545
ACS Chem. Neurosci. 2019, 10, 1603−1614

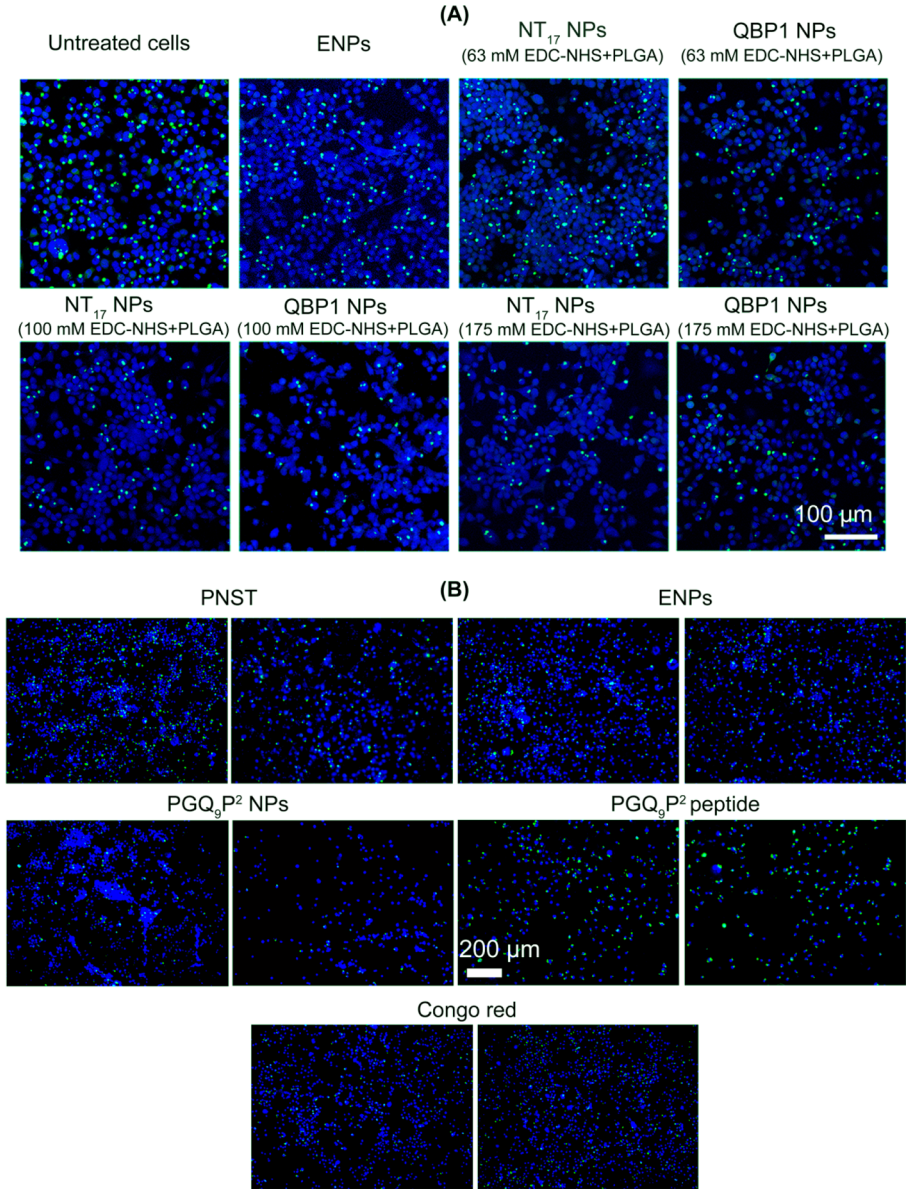

Figure 3. Representative microscopic images of Neuro 2A cells under the influence of various treatments (Ponasterone A, peptide inhibitors, empty nanoparticles, and peptide inhibitor loaded nanoparticles).

brain sections revealed distinct red fluorescence of PLGA-Neutral red nanoparticles (Figure 2E) which confirms the transfer of nanoparticles across the BBB. Overall, in vitro and in vivo translocation studies of fluorescent PLGA nanoparticles suggest successful polysorbate 80 mediated brain delivery.

In Vitro Efficacy of Peptide Loaded Nanoparticles in Neuro 2A Cells and PC12 Cells. An ideal delivery system should release the drug in controlled way at the targeted site which would exert the intended action against the pathological mechanism. For the study of efficacy of peptide loaded PLGA NPs, the best system could have been coculture model of MDCK cells and Neuro 2A cells as a representation of BBB and HD conditions. However, the coculture experiments were unsuccessful owing to technical difficulties such as low TEER values (~50 $\Omega \cdot cm^2$), submaximal differentiation of Neuro 2A cells, and faster depletion of nutrients from Dulbecco's modified Eagle's medium (as evident from medium color). Thus, in an alternate approach, using two different cell models – (i) Neuro-2A cells expressing truncated N-terminal of mutant huntingtin with pathogenic polyglutamine tract (150Qs) fused with enhanced green fluorescent protein (EGFP) [tNhtt-150Q-EGFP][31] and (ii) PC12 cells expressing huntingtin exon1 with pathogenic polyglutamine tract (74Qs) fused with EGFP [HD-Q74-EGFP],[32] the efficacy of PGQ_9P^2, QBP1, and NT_{17} loaded nanoparticles was analyzed separately. First, ponasterone A (PNST) dose dependent expression of tNhtt-150Q-EGFP in Neuro 2A cells and doxycycline (Dox) dose dependent expression of HD-Q74-EGFP in PC12 cells was confirmed and found to corroborate with previous reports (Figures S7–S10).[31] Based on expression and aggregate levels, 10 μM PNST and 1000 ng/mL Dox were used in further experiments. To assess the efficacy of PGQ_9P^2-NPs, QBP1-NPs, and NT_{17}-NPs, the treatment was given as shown in Table S2. Along with only solvents, peptide inhibitors (without nanoformulations), and ENPs, we have also used a known inhibitor of polyglutamine aggregation, Congo red (100 μM), as a positive control (Table S2).[33]

DOI: 10.1021/acschemneuro.8b00545
ACS Chem. Neurosci. 2019, 10, 1603−1614

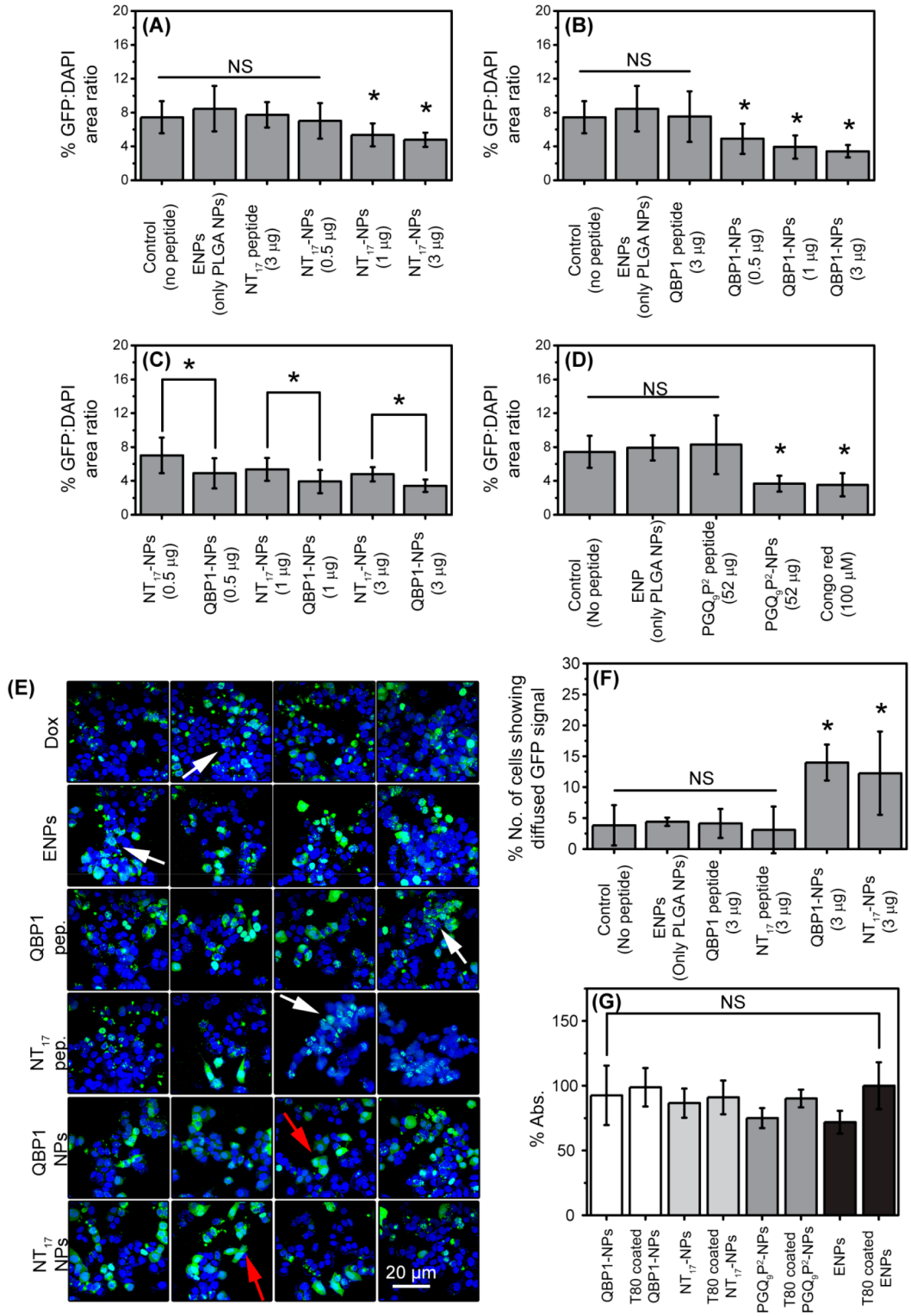

Figure 4. Quantification of effect of (A) NT_{17}-NPs and (B) QBP1-NPs treatment in comparison with untreated, ENPs treated, and only peptide inhibitors (without nanoformulations) in Neuro 2A cells. (C) Comparison between effect of NT_{17}-NPs and QBP1-NPs. (D) Quantification of effect of PGQ_9P^2-NPs treatment in comparison with various control groups in Neuro 2A cells. [Asterisk (*) in A–D indicates significantly different observations, ANOVA on the ranks, p-value < 0.05. NS indicates no significant difference.] (E) Representative confocal microscopy images of PC12 cells treated with only Dox, ENPs, peptide inhibitors, NT_{17}-NPs, and QBP1-NPs. (F) Quantification of effect various treatments (ENPs, NT_{17} peptide, QBP1 peptide, NT_{17}-NPs, and QBP1-NPs) on PC12 cells. [Asterisk (*) in F indicates significantly different observations, ANOVA on the ranks, p-value < 0.05. NS indicates no significant difference.] (G) Cytotoxicity assay performed in Neuro 2A cells using uncoated and polysorbate 80 coated nanoparticles. [NS indicates no significant difference.]

The inhibition of tNhtt-150Q-EGFP aggregation in Neuro 2A cells can be observed as the reduction in EGFP tagged green fluorescent aggregates[34,35] (Figure 3). In the case of NT_{17}-NPs, significant inhibition was obtained only at

DOI: 10.1021/acschemneuro.8b00545
ACS Chem. Neurosci. 2019, 10, 1603–1614

intermediate and high (1 and 3 μg) peptide load (ANOVA on the ranks, p-value < 0.05) as compared to ENPs treated and untreated cells (Figures 3A and 4A). NT_{17} molecules, after their inclusion into α-helical bundles formed by aggregation prone N-terminal fragments of mutant huntingtin, decrease local concentration of PolyQ within oligomeric structures, leading to reduction in their interactions, and thereby inhibit nucleation within oligomeric structures of N-terminal fragments.[12] The probable reason for failure of NT_{17}-NPs to inhibit aggregation at the lowest peptide load (0.5 μg) could be the insufficient number of molecules in the vicinity of growing aggregates of tNhtt-150Q-EGFP. But, as the number of NT_{17} molecules increased at intermediate and high concentrations, significant inhibition was observed. Unlike NT_{17}-NPs, QBP1-NPs show statistically significant inhibition of tNhtt-150Q-EGFP aggregation at all selected levels of peptide load (ANOVA on the ranks, p-value < 0.05) (Figures 3A and 4B). It has been reported that "WKWW" motif of the QBP1 peptide has a tendency to interact and bind with PolyQ strongly which leads to inhibition of oligomerization and elongation.[13,36,37] QBP1 has the highest binding capacity among all QBP variants.[13,36] Thus, we speculate that, because of high binding capacity,[13,36] it inhibited tNhtt-150Q-EGFP aggregation in the cells even at low concentration. Comparison between effects of NT_{17}-NPs and QBP1-NPs showed significant difference at all dose levels which suggests that QBP1 peptide has more pronounced aggregation inhibitory potential than NT_{17} (Figure 4C). In a separate experiment, PGQ_9P^2-NPs also showed significant reduction in the number of aggregate positive cells as compared to the PGQ_9P^2 peptide and ENPs treatment (one-way ANOVA, p-value < 0.05) (Figures 3B and 4D). The effect was statistically equivalent to that of Congo red which is a known inhibitor of amyloid aggregation. PGQ_9P^2 acts on elongation phase of polyglutamine aggregation.[11] Because of the proline residue in middle of second Q_9 sequence (Table 1), this peptide does not aggregate in vitro.[11,38] Additionally, the side chain of proline disfavors its accommodation in a growing beta strand.[11] Owing to these properties of PGQ_9P^2 and prohibition of addition of another polyglutamine molecule in the growing fibril leads to inhibition of the elongation phase of polyglutamine aggregation.[11] Due to the unavailability of the PGQ_9P^2 peptide, we have used QBP1-NPs and NT_{17}-NPs for further experiments. As QBP1-NPs and NT_{17}-NPs with highest peptide load showed maximum inhibitory effect against aggregation in Neuro 2A cells, these nanoparticles were tested in PC12 cell model of HD (Figure 4E). In PC12 cells, treatment with ENPs and peptide inhibitors (without nanoformulation) led to appearance of green fluorescent puncta with no/minimal number of cells showing diffused EGFP fluorescence (Figure 4E, white arrows) similar to the case of untreated cells. But, after treatment with QBP1-NPs and NT_{17}-NPs, diffused green fluorescence was observed in the cytoplasm of PC12 cells (Figure 4, E, red arrows). It represents the inhibition of HD-Q74-EGFP aggregation which is in agreement with previous reports.[32,39,40] We believe that QBP1 and NT_{17}, present in the vicinity, prevent formation of the insoluble aggregates. Therefore, the cells show the presence of a nonaggregated and soluble fraction of HD-Q74-EGFP that can be observed as diffused green fluorescence spread across the cytoplasm. After analyzing multiple images, it was found that QBP1-NPs and NT_{17}-NPs treated cells show significant inhibition as compared to all control groups (ANOVA on the ranks, p-value < 0.05) (Figure 4F). Overall results suggest that the peptide inhibitors, when delivered via PLGA nanoparticles, showed significant inhibition in both cell models. The reason for reduction in aggregates and increased EGFP diffused signal can be sought out from "aggresome and degrasome" theory[41,42] (Figure 6). It has been shown that proteins with expanded PolyQ (tNhtt-150Q-EGFP in Neuro 2A cells and HD-Q74-EGFP in PC12 cells) are prone to aggregation.[31,32] In response to expression and early aggregation of these fragments, cells recruit several chaperone members and ubiquitin-proteasomal system (UPS).[43] These chaperone members and UPS promote refolding of the misfolded protein fragment, and its transport and degradation in a cell organelle called "degrasome" (Figure 6). Previous reports suggest that cells express chaperone members from Hsp 40 and 70 families in a PolyQ length dependent manner which eventually degrade mutant protein fragments.[44−46] The expanded PolyQ sequence (150 Qs in Neuro 2A cells and 74 Qs in PC12 cells) shows resistance to the degradation, leading to the accumulation and colocalization of chaperone members in insoluble aggregates of tNhtt-150Q-EGFP and HD-Q74-EGFP.[44−46] At this stage, the "degrasome" is converted to "aggresome" which appears as a distinct green fluorescent aggregates in Neuro 2A and granular puncta in PC12 cells (Figure 6). However, we believe that the treatment with PGQ_9P^2-NPs, QBP1-NPs, and NT_{17}-NPs leads to inhibition of polyglutamine aggregation which facilitates the degradation of fragments during early aggregation events. The removal of mutant protein fragments finally results in the loss of green fluorescence in Neuro 2A cells[44−47] (Figure 6). It has been reported that, in PC12 cells, the mutant huntingtin is cleared out slowly over time by either autophagy or UPS.[47−49] We propose that, due to slow clearance of HD-Q74-EGFP, it is possible to observe the diffused signal in PC12 cells, which otherwise, on continuation of experiment, would probably be lost over time[47−49] (Figure 6). The peptide loaded nanoparticles prevent the aggregate formation which can be observed as increased soluble fraction of HD-Q74-EGFP and increased diffused green fluorescence across the PC12 cell cytoplasm. However, to prove this theory, extensive experiments are needed to determine the expression and colocalization of each chaperone member before and after treatment with peptide inhibitor loaded nanoparticles.

Efficacy of QBP1-NPs and NT_{17}-NPs in *Drosophila* Model of HD. Among many animal models of HD, rodent models (R6/1, R6/2, and YAC128 mice) are widely used due to closeness of molecular mechanism of HD neuropathology to human HD patients.[50,51] However, higher PolyQ length (112−144) hastens the disease progression, making them severe HD models.[51] Also, the cost of maintenance, feeding, and breeding the rodent models is very high.[50,52,53] On the other hand, fly models are also widely used to study Huntington's disease because of their specialized nervous system that is linked with functions of memory, cognition, olfaction, and vision.[52,53] *Drosophila* also expresses huntingtin protein which has homologous sequence to human huntingtin at five different regions.[53] Easier methods for tweaking the genetic architecture, low maintenance cost, easier handling, and short life span make these fly models very useful in initial drug and drug delivery screening.[52,53] Hence, in order to gain preliminary proof for the efficacy of peptide loaded nanoparticles, flies containing the HD gene with pathogenic PolyQ (*Elav-GAL4*>UAS-httex1pQ93 and referred as Q93 larvae/flies)[54,55] and control flies with normal PolyQ (*Elav-*

DOI: 10.1021/acschemneuro.8b00545
ACS Chem. Neurosci. 2019, 10, 1603−1614

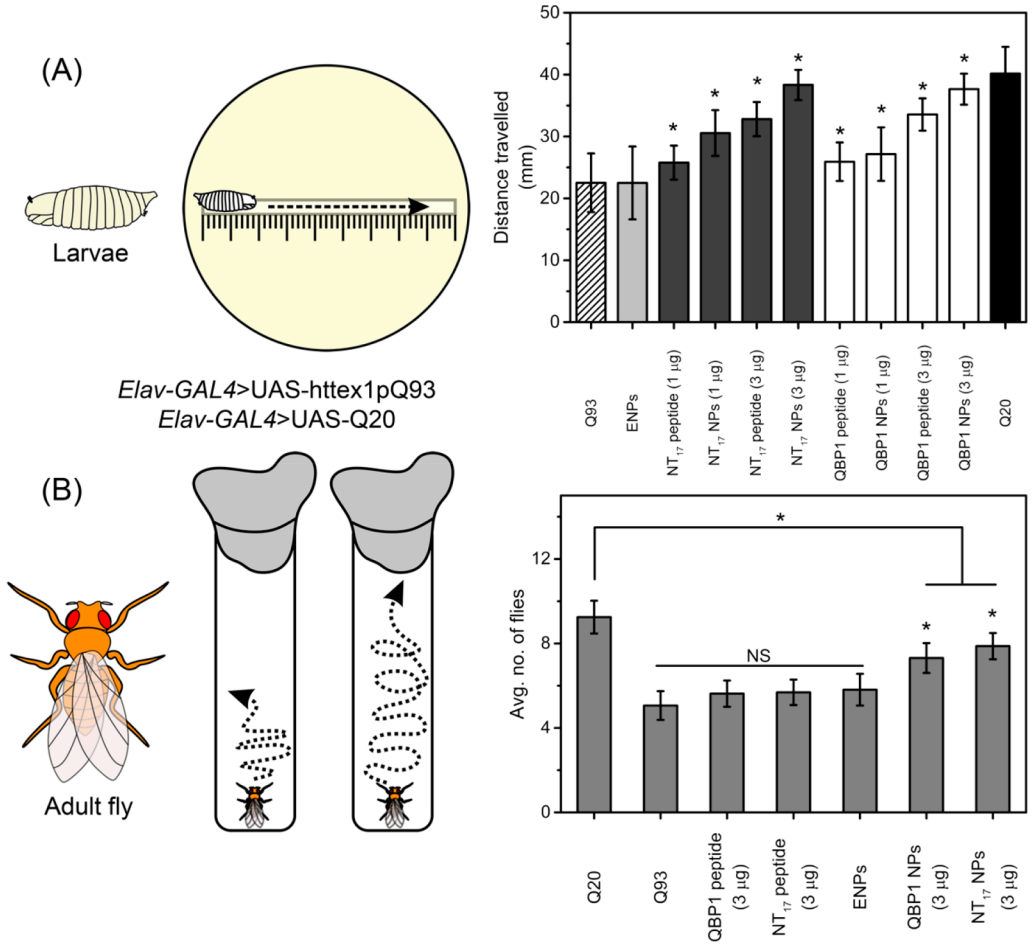

Figure 5. (A) Crawling assay performed using third instar larvae in an agar plate having a groove of fixed measurements. (B) Climbing assay performed using adult flies (age: 10th day from eclosion) in vertical transparent tubes. [Asterisk (*) in A and B indicates significantly different observations, ANOVA on the ranks, p-value < 0.05. NS indicates no significant difference.]

GAL4>UAS-Q20 and referred as Q20 larvae/flies)[55,56] were used. In *Drosophila*, the neuronal circuits and synapses develop in late embryonic stage. In third instar larvae, all 11 segments (3 thoracic and 8 abdominal) are supplied by motor neurons which form neuromuscular junctions with larval muscles. The expression system (*Elav-GAL4*>UAS-httex1pQ93 and *Elav-GAL4*>UAS-Q20) in our *Drosophila* experiments shows pan-neuronal expression of the HD gene (Q93) and control gene (Q20). Therefore, Q93 expression and its aggregation in the motor neurons directly affect the crawling behavior of the third instar larvae.[57] In Q20 larvae, normal crawling activity is expected as neurodegeneration is absent.[57] Similarly, the adult flies grown from the Q93 larvae show advanced neuro-degeneration and poor neuronal development which further culminates into reduced climbing activity, whereas the flies grown from Q20 larvae show normal climbing activity.[57] In our experiments, crawling activity was significantly higher for Q93 larvae fed with NT_{17} and QBP1 peptides (without nano-formulation) at low (~1 μg) and high (~3 μg) amounts as compared to untreated and ENP treated groups (ANOVA on the ranks, p-value < 0.05). The groups of larvae fed with QBP1-NPs and NT_{17}-NPs bearing similar peptide load showed even higher crawling activity that was significantly different (ANOVA on the ranks, p-value < 0.05) from the groups fed with ENPs and peptides without nanoformulation (Figure 5A). The nanoparticles with higher peptide load (~3 μg) showed comparable crawling activity (no significant difference, ANOVA on the ranks, p-value > 0.05) to control larvae (Q20) (Figure 5A). Based on these results, we selected nanoparticles with the highest peptide load (~3 μg) for climbing assay. When Q93 flies were fed with peptides (without nanoformulation), no significant climbing activity was observed as compared to untreated and ENPs treated flies (ANOVA on the ranks, p-value > 0.05) (Figure 5B). The average number of flies reaching 7 cm distance was low for untreated flies, ENPs treated flies, and peptide inhibitor treated (without nanoparticulate formulations) flies (Figure 5B). However, the flies fed with nanoparticles bearing similar peptide load (~3 μg) showed significantly higher climbing activity (ANOVA on the ranks, p-value < 0.05) (Figure 5B).

To summarize, the nanoparticles with low and high peptide load (1 and 3 μg of NT_{17} and QBP1) showed significant improvement in motor performance at the larval stage of *Drosophila*. Highest peptide load (3 μg) also showed improvement in climbing activity in adult flies. We presume that NT_{17} and QBP1 peptides have limited half-life in larvae and adult flies. But, the nanoparticles prevented in vivo degradation of QBP1 and NT_{17} peptides during their transit to the site of aggregation. Hence, the effective amount of peptide inhibitors, available in vivo for the inhibition of aggregation, is probably higher as compared to peptides alone (Figure 6). This led to reduced degeneration of motor neurons, and hence,

DOI: 10.1021/acschemneuro.8b00545
ACS Chem. Neurosci. 2019, 10, 1603−1614

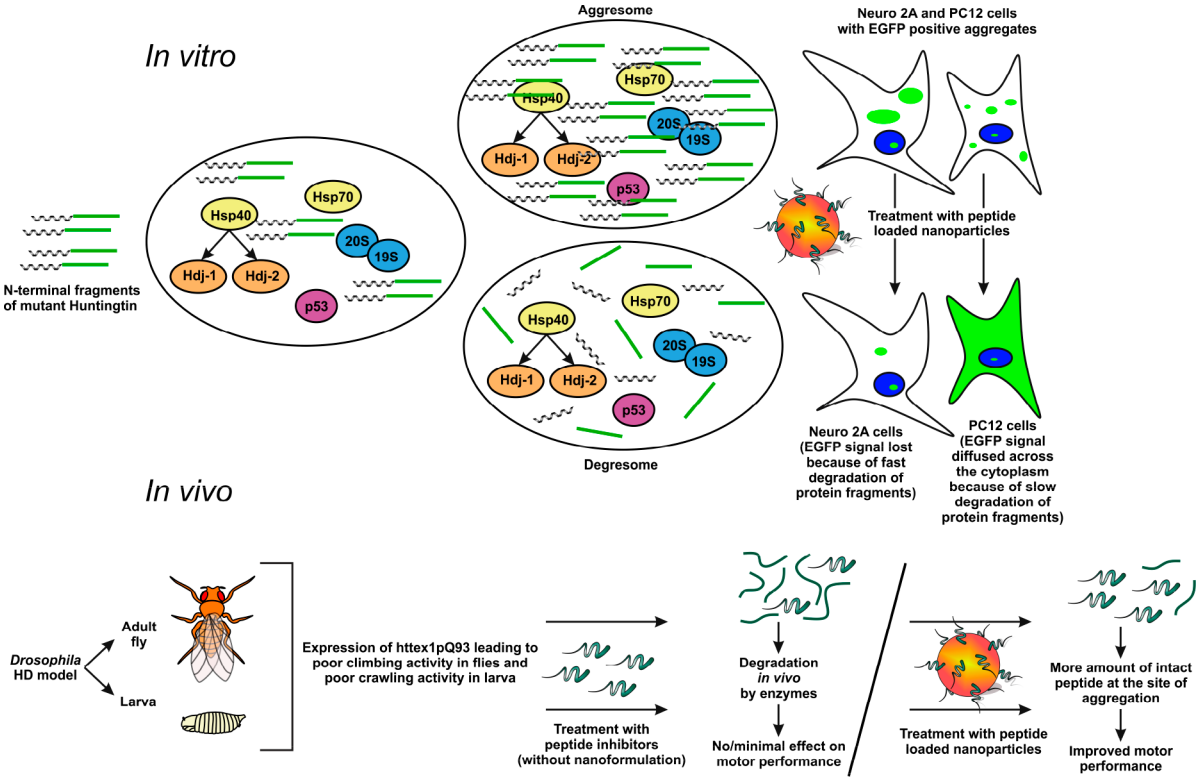

Figure 6. Schematic showing hypothesis behind (A) inhibition of polyglutamine aggregation in Neuro 2A cells and PC12 cell models of HD by peptide loaded nanoparticles and (B) inhibition of aggregation and improvement in motor performance of *Drosophila* model of HD (at larval and adult stage).

higher crawling activity in larvae and higher climbing activity in flies were observed after nanoparticles treatment. We observed dose dependent motor improvement in larvae and flies (Figure 5, A). But, the climbing activity of Q93 flies treated with QBP1-NPs and NT_{17}-NPs is significantly low (ANOVA on the ranks, p-value < 0.05) as compared to control flies (Q20) (Figure 5B). This suggests that the selected dose of peptide inhibitors shows submaximal improvement in locomotion of adult flies. We propose that improving dose levels of both QBP1-NPs and NT_{17}-NPs may result in maximum climbing activity. Overall, both QBP1-NPs and NT_{17}-NPs led to improvement in motor activity in *Drosophil*a model of HD.

Biocompatibility and Biosafety of ENPs, Peptide Loaded Nanoparticles, and Fluorescent Nanoparticles. It is essential for any drug delivery system to be biodegradable, biocompatible, and safe for passing the regulatory requirements in preclinical and clinical setups. First, the cytotoxicity was elucidated using in vitro 3-(4,5-dimethythiazol-2-yl)-2,5-diphenyl tetrazolium bromide (MTT) assay[S8] which showed no significant cell death in any experimental group (one-way ANOVA, p-value > 0.05, Figure 4G). This suggests that the uncoated and polysorbate 80 coated nanoparticles are not cytotoxic at the selected concentrations. Further, no significant cell death was seen in Neuro 2A as well as PC12 cells in peptide efficacy experiments. Additionally, in the BBB model, nanoparticles did not cause cell death or monolayer rupture during transcytosis. Furthermore, hematoxylin and eosin (H&E) staining[S9,60] of the tissue samples that were collected and processed after intravenous administration of nanoparticle suspension in healthy mice revealed no necrotic or apoptotic features (Figure S11). Also, we did not observe significant death in *Drosophila* larvae and adult flies while nurturing and performing crawling and climbing assays. Collectively, these results confirm in vitro and in vivo biocompatibility of empty, fluorescent, and peptide loaded PLGA nanoparticles.

CONCLUSION

Polyglutamine aggregation is believed to be a fundamental problem of HD. The understanding of the molecular basis of HD neuropathology has revealed polyglutamine aggregation as one of the potential targets that can be inhibited by novel mechanism based peptide inhibitors. But the physiologically tough BBB and short in vivo half-life may hinder their preclinical testing in higher animal models. Hence, we have synthesized PLGA nanoparticles containing PGQ_9P^2, QBP1, and NT_{17} peptides. We used nanoprecipitation method for physical encapsulation of PGQ_9P^2 peptide[20] and carbodiimide cross-linking method followed by nanoprecipitation for QBP1 and NT_{17} peptides. The peptide loaded nanoparticles were characterized by DLS, SEM, and ATR-FTIR. The highly sensitive ATR-FTIR method confirmed PLGA activation by carbodiimide chemistry, its products, conjugation of peptides, and their probable structural features in the nanoparticles. The transcytosis experiments performed using the in vitro BBB model of MDCK cells and the biodistribution study in healthy mice revealed polysorbate 80 mediated translocation of fluorescent PLGA nanoparticles across the BBB. The peptide loaded nanoparticles displayed dose dependent inhibition of polyglutamine aggregation in Neuro 2A and PC12 cell models of HD and improved motor performance in the *Drosophila* model of HD. Additionally, no cell death, no microscopic tissue toxicity in healthy mice, and no larval/fly death in any of experimental groups confirmed biocompatibility and biosafety of the nanoparticulate formulations. Collectively, our findings

DOI: 10.1021/acschemneuro.8b00545
ACS Chem. Neurosci. 2019, 10, 1603−1614

show a successful attempt of delivery of PLGA nanoparticles containing three peptide inhibitors and their efficacy in cell models and the *Drosophila* model of HD. We believe that these results will be helpful in designing future studies in higher animal models to test the peptide inhibitor loaded PLGA nanoparticles in HD and other polyglutamine expansion related diseases.

METHODS

All materials and methods are provided in the Supporting Information.

ASSOCIATED CONTENT

Supporting Information

The Supporting Information is available free of charge on the ACS Publications website at DOI: 10.1021/acschemneuro.8b00545.

All materials and methods including statistical analysis, tables, and figures along with supporting text and references (PDF)

AUTHOR INFORMATION

ORCID

Abhayraj S. Joshi: 0000-0003-4161-5207
Virender Singh: 0000-0002-6720-8784
Ashwani Kumar Thakur: 0000-0002-7268-6836

Author Contributions

A.S.J. and A.K.T. planned all experiments related to nanoparticle design, synthesis and characterization. A.S.J. performed all experiments related to nanoparticles design, synthesis, and characterization. A.S.J. established and optimized the cell culture protocol related to in vitro BBB model (MDCK cells) and cell models of HD (Neuro 2A cells and PC12 cells). A.S.J. and A.Y.G. designed, optimized, and performed all in vivo experiments using healthy mice. V.S. designed, optimized, and performed all in vivo experiments using the *Drosophila* model of HD. A.S.J. and A.K.T. discussed and analyzed the data. A.S.J and A.K.T. wrote the manuscript. A.K.T. provided direction and supervision for the project. All authors critically discussed and approved the final draft of the manuscript.

Funding

This work was supported by the Department of Science and Technology (DST), Government of India, India [Grant number: DST/BSBE/2016156].

Notes

The authors declare the following competing financial interest(s): The authors would like to declare conflict of interest according to the provisional patent application number 201811024748.

ACKNOWLEDGMENTS

We are grateful to Dr. Nihar Ranjan Jana (National Brain Research Centre (NBRC), India) and Dr. David C. Rubinsztein (Cambridge Institute for Medical Research (CIMR), U.K.) for providing Neuro 2A and PC12 cell models of HD for this work. We are thankful to Dr. Sarvanan (Department of Biological Sciences and Bioengineering, IIT Kanpur) and Dr. Sovan Das (Department of Mechanical Engineering, IIT Kanpur) for confocal microscopy facility. We are grateful to Prof. S. C. Lakhotia and Prof. Namita Agarwal for providing us *Drosophila* stock for in vivo work. We convey our sincere gratitude to Dr. Pradip Sinha and Mr. Thamarai for providing lab space and all help for our in vivo experiments.

ABBREVIATIONS USED

ApoE, apolipoprotein E; ATR-FTIR, attenuated total reflectance-Fourier transform infrared spectroscopy; BBB, blood-brain barrier; cAMP, cyclic adenosine monophosphate; DAPI, 4′,6-diamidino-2-phenylindole; dbcAMP, N6,2′-*O*-dibutyryladenosine-3′,5′-cyclic monophosphate; DLS, dynamic light scattering; DMEM, Dulbecco's modified Eagle's medium; Dox, doxycycline; EDC, 1-ethyl-3-(3-dimethylaminopropyl) carbodiimide; EGFP, enhanced green fluorescent protein; ENPs, empty nanoparticles; FBS, fetal bovine serum; FD, fluorescein isothiocyanate-Dextran 40000; FI, fluorescein isothiocyanate-Inulin; FITC, fluorescein isothiocyanate; HD, Huntington's disease; HS, horse serum; LDL, low density lipoproteins; MDCK, Madin-Darby canine kidney cells; mHtt, mutant huntingtin protein; MTT, 3-(4,5-dimethylthiazol-2-yl)-2,5-diphenyltetrazolium bromide; NHS, *N*-hydroxysuccinimide; NPs, nanoparticles; PDI, polydispersity index; PLGA, poly-D,L-lactide-*co*-glycolide; PNST, ponasterone A; PolyQ, polyglutamine; PTFE, polytetrafluoroethylene; RP-HPLC, reversed-phase high-performance liquid chromatography; TEER, trans-endo/epithelial electrical resistance; tNhtt, truncated N-terminal fragment of mutant human huntingtin (1−90 amino acids); ZP, zeta potential; ZO-1, Zonula occludens-1 protein

REFERENCES

(1) Zuccato, C., Valenza, M., and Cattaneo, E. (2010) Molecular mechanisms and potential therapeutical targets in Huntington's disease. *Physiol. Rev. 90*, 905−981.

(2) MacDonald, M. E., Ambrose, C. M., Duyao, M. P., Myers, R. H., Lin, C., Srinidhi, L., Barnes, G., Taylor, S. A., James, M., Groot, N., MacFarlane, H., Jenkins, B., Anderson, M. A., Wexler, N. S., Gusella, J. F., Bates, G. P., Baxendale, S., Hummerich, H., Kirby, S., North, M., Youngman, S., Mott, R., Zehetner, G., Sedlacek, Z., Poustka, A., Frischauf, A.-M., Lehrach, H., Buckler, A. J., Church, D., Doucette-Stamm, L., O'Donovan, M. C., Riba-Ramirez, L., Shah, M., Stanton, V. P., Strobel, S. A., Draths, K. M., Wales, J. L., Dervan, P., Housman, D. E., Altherr, M., Shiang, R., Thompson, L., Fielder, T., Wasmuth, J. J., Tagle, D., Valdes, J., Elmer, L., Allard, M., Castilla, L., Swaroop, M., Blanchard, K., Collins, F. S., Snell, R., Holloway, T., Gillespie, K., Datson, N., Shaw, D., and Harper, P. S. (1993) A novel gene containing a trinucleotide repeat that is expanded and unstable on Huntington's disease chromosomes. *Cell 72*, 971−983.

(3) Thakur, A. K., Jayaraman, M., Mishra, R., Thakur, M., Chellgren, V. M., Byeon, I. J., Anjum, D. H., Kodali, R., Creamer, T. P., Conway, J. F., Gronenborn, A. M., and Wetzel, R. (2009) Polyglutamine disruption of the huntingtin exon 1 N terminus triggers a complex aggregation mechanism. *Nat. Struct. Mol. Biol. 16*, 380−389.

(4) Ross, C. A., Poirier, M. A., Wanker, E. E., and Amzel, M. (2003) Polyglutamine fibrillogenesis: The pathway unfolds. *Proc. Natl. Acad. Sci. U. S. A. 100*, 1−3.

(5) Graham, R. K., Deng, Y., Slow, E. J., Haigh, B., Bissada, N., Lu, G., Pearson, J., Shehadeh, J., Bertram, L., Murphy, Z., Warby, S. C., Doty, C. N., Roy, S., Wellington, C. L., Leavitt, B. R., Raymond, L. A., Nicholson, D. W., and Hayden, M. R. (2006) Cleavage at the caspase-6 site is required for neuronal dysfunction and degeneration due to mutant huntingtin. *Cell 125*, 1179−1191.

(6) Todd, T. W., and Lim, J. (2013) Aggregation Formation in the Polyglutamine Diseases: Protection at a Cost? *Mol. Cells 36*, 185−194.

(7) Rodrigues, F. B., Duarte, G. S., Costa, J., Ferreira, J. J., and Wild, E. J. (2017) Tetrabenazine Versus Deutetrabenazine for Huntington's Disease: Twins or Distant Cousins? *Movement Disorders Clinical Practice 4*, 582−585.

DOI: 10.1021/acschemneuro.8b00545
ACS Chem. Neurosci. 2019, 10, 1603−1614

(8) Sah, D. W. Y., and Aronin, N. (2011) Oligonucleotide therapeutic approaches for Huntington disease. *J. Clin. Invest. 121*, 500−507.
(9) Fecke, W., Gianfriddo, M., Gaviraghi, G., Terstappen, G. C., and Heitz, F. (2009) Small molecule drug discovery for Huntington's Disease. *Drug Discovery Today 14*, 453−464.
(10) Takeuchi, T., Popiel, H. A., Futaki, S., Wada, K., and Nagai, Y. (2014) Peptide-based therapeutic approaches for treatment of the polyglutamine diseases. *Curr. Med. Chem. 21*, 2575−2582.
(11) Thakur, A. K., Yang, W., and Wetzel, R. (2004) Inhibition of polyglutamine aggregate cytotoxicity by a structure-based elongation inhibitor. *FASEB J. 18*, 923−925.
(12) Mishra, R., Jayaraman, M., Roland, B. P., Landrum, E., Fullam, T., Kodali, R., Thakur, A. K., Arduini, I., and Wetzel, R. (2012) Inhibiting the nucleation of amyloid structure in a huntingtin fragment by targeting alpha-helix-rich oligomeric intermediates. *J. Mol. Biol. 415*, 900−917.
(13) Nagai, Y., Tucker, T., Ren, H., Kenan, D. J., Henderson, B. S., Keene, J. D., Strittmatter, W. J., and Burke, J. R. (2000) Inhibition of polyglutamine protein aggregation and cell death by novel peptides identified by phage display screening. *J. Biol. Chem. 275*, 10437−10442.
(14) Arribat, Y., Bonneaud, N., Talmat-Amar, Y., Layalle, S., Parmentier, M. L., and Maschat, F. (2013) A huntingtin peptide inhibits polyQ-huntingtin associated defects. *PLoS One 8*, e68775.
(15) Tang, T.-S., Guo, C., Wang, H., Chen, X., and Bezprozvanny, I. (2009) Neuroprotective effects of inositol 1,4,5-trisphosphate receptor carboxy-terminal fragment in Huntington's disease mouse model. *J. Neurosci. 29*, 1257−1266.
(16) Dudek, N. L., Dai, Y., and Muma, N. A. (2010) Neuroprotective Effects of Calmodulin Peptide 76−121aa: Disruption of Calmodulin Binding to Mutant Huntingtin. *Brain Pathol. 20*, 176−189.
(17) Martin, B., Golden, E., Carlson, O. D., Pistell, P., Zhou, J., Kim, W., Frank, B. P., Thomas, S., Chadwick, W. A., Greig, N. H., Bates, G. P., Sathasivam, K., Bernier, M., Maudsley, S., Mattson, M. P., and Egan, J. M. (2009) Exendin-4 Improves Glycemic Control, Ameliorates Brain and Pancreatic Pathologies, and Extends Survival in a Mouse Model of Huntington's Disease. *Diabetes 58*, 318−328.
(18) Hafner, A., Lovric, J., Lakos, G. P., and Pepic, I. (2014) Nanotherapeutics in the EU: an overview on current state and future directions. *Int. J. Nanomed. 9*, 1005−1023.
(19) Arribat, Y., Talmat-Amar, Y., Paucard, A., Lesport, P., Bonneaud, N., Bauer, C., Bec, N., Parmentier, M.-L., Benigno, L., Larroque, C., Maurel, P., and Maschat, F. (2014) Systemic delivery of P42 peptide: a new weapon to fight Huntington's disease. *Acta Neuropathologica Communications 2*, 86.
(20) Joshi, A. S., and Thakur, A. K. (2014) Biodegradable delivery system containing a peptide inhibitor of polyglutamine aggregation: a step toward therapeutic development in Huntington's disease. *J. Pept. Sci. 20*, 630−639.
(21) Koffie, R. M., Farrar, C. T., Saidi, L. J., William, C. M., Hyman, B. T., and Spires-Jones, T. L. (2011) Nanoparticles enhance brain delivery of blood-brain barrier-impermeable probes for in vivo optical and magnetic resonance imaging. *Proc. Natl. Acad. Sci. U. S. A. 108*, 18837−18842.
(22) Valetti, S., Mura, S., Noiray, M., Arpicco, S., Dosio, F., Vergnaud, J., Desmaele, D., Stella, B., and Couvreur, P. (2014) Peptide conjugation: before or after nanoparticle formation? *Bioconjugate Chem. 25*, 1971−1983.
(23) Zhang, N., Chittasupho, C., Duangrat, C., Siahaan, T. J., and Berkland, C. (2008) PLGA Nanoparticle-Peptide Conjugate Effectively Targets Intercellular Cell-Adhesion Molecule-1. *Bioconjugate Chem. 19*, 145−152.
(24) Costantino, L., Gandolfi, F., Tosi, G., Rivasi, F., Vandelli, M. A., and Forni, F. (2005) Peptide-derivatized biodegradable nanoparticles able to cross the blood−brain barrier. *J. Controlled Release 108*, 84−96.
(25) Moghimi, S. M., Hunter, A. C., and Murray, J. C. (2001) Long-circulating and target-specific nanoparticles: theory to practice. *Pharmacol. Rev. 53*, 283−318.
(26) Wohlfart, S., Gelperina, S., and Kreuter, J. (2012) Transport of drugs across the blood-brain barrier by nanoparticles. *J. Controlled Release 161*, 264−273.
(27) Yu, D., Zou, G., Cui, X., Mao, Z., Estrela-Lopis, I., Donath, E., and Gao, C. (2015) Monitoring the intracellular transformation process of surface-cleavable PLGA particles containing disulfide bonds by fluorescence resonance energy transfer. *J. Mater. Chem. B 3*, 8865−8873.
(28) Koffie, R. M., Farrar, C. T., Saidi, L.-J., William, C. M., Hyman, B. T., and Spires-Jones, T. L. (2011) Nanoparticles enhance brain delivery of blood−brain barrier-impermeable probes for in vivo optical and magnetic resonance imaging. *Proc. Natl. Acad. Sci. U. S. A. 108*, 18837−18842.
(29) Dsouza, R. N., Pischel, U., and Nau, W. M. (2011) Fluorescent Dyes and Their Supramolecular Host/Guest Complexes with Macrocycles in Aqueous Solution. *Chem. Rev. 111*, 7941−7980.
(30) Vergoni, A. V., Tosi, G., Tacchi, R., Vandelli, M. A., Bertolini, A., and Costantino, L. (2009) Nanoparticles as drug delivery agents specific for CNS: in vivo biodistribution. *Nanomedicine 5*, 369−377.
(31) Wang, G. H., Mitsui, K., Kotliarova, S., Yamashita, A., Nagao, Y., Tokuhiro, S., Iwatsubo, T., Kanazawa, I., and Nukina, N. (1999) Caspase activation during apoptotic cell death induced by expanded polyglutamine in N2a cells. *NeuroReport 10*, 2435−2438.
(32) Wyttenbach, A., Swartz, J., Kita, H., Thykjaer, T., Carmichael, J., Bradley, J., Brown, R., Maxwell, M., Schapira, A., Orntoft, T. F., Kato, K., and Rubinsztein, D. C. (2001) Polyglutamine expansions cause decreased CRE-mediated transcription and early gene expression changes prior to cell death in an inducible cell model of Huntington's disease. *Hum. Mol. Genet. 10*, 1829−1845.
(33) Sanchez, I., Mahlke, C., and Yuan, J. (2003) Pivotal role of oligomerization in expanded polyglutamine neurodegenerative disorders. *Nature 421*, 373−379.
(34) Bauer, P. O., Wong, H. K., Oyama, F., Goswami, A., Okuno, M., Kino, Y., Miyazaki, H., and Nukina, N. (2009) Inhibition of Rho kinases enhances the degradation of mutant huntingtin. *J. Biol. Chem. 284*, 13153−13164.
(35) Debnath, K., Shekhar, S., Kumar, V., Jana, N. R., and Jana, N. R. (2016) Efficient Inhibition of Protein Aggregation, Disintegration of Aggregates, and Lowering of Cytotoxicity by Green Tea Polyphenol-Based Self-Assembled Polymer Nanoparticles. *ACS Appl. Mater. Interfaces 8*, 20309−20318.
(36) Ren, H., Nagai, Y., Tucker, T., Strittmatter, W. J., and Burke, J. R. (2001) Amino acid sequence requirements of peptides that inhibit polyglutamine-protein aggregation and cell death. *Biochem. Biophys. Res. Commun. 288*, 703−710.
(37) Nagai, Y., Fujikake, N., Ohno, K., Higashiyama, H., Popiel, H. A., Rahadian, J., Yamaguchi, M., Strittmatter, W. J., Burke, J. R., and Toda, T. (2003) Prevention of polyglutamine oligomerization and neurodegeneration by the peptide inhibitor QBP1 in Drosophila. *Hum. Mol. Genet. 12*, 1253−1259.
(38) Thakur, A. K., and Wetzel, R. (2002) Mutational analysis of the structural organization of polyglutamine aggregates. *Proc. Natl. Acad. Sci. U. S. A. 99*, 17014−17019.
(39) Ravikumar, B., Stewart, A., Kita, H., Kato, K., Duden, R., and Rubinsztein, D. C. (2003) Raised intracellular glucose concentrations reduce aggregation and cell death caused by mutant huntingtin exon 1 by decreasing mTOR phosphorylation and inducing autophagy. *Hum. Mol. Genet. 12*, 985−994.
(40) Apostol, B. L., Kazantsev, A., Raffioni, S., Illes, K., Pallos, J., Bodai, L., Slepko, N., Bear, J. E., Gertler, F. B., Hersch, S., Housman, D. E., Marsh, J. L., and Thompson, L. M. (2003) A cell-based assay for aggregation inhibitors as therapeutics of polyglutamine-repeat disease and validation in Drosophila. *Proc. Natl. Acad. Sci. U. S. A. 100*, 5950−5955.
(41) Mishra, A., Godavarthi, S. K., Maheshwari, M., Goswami, A., and Jana, N. R. (2009) The Ubiquitin Ligase E6-AP Is Induced and

DOI: 10.1021/acschemneuro.8b00545
ACS Chem. Neurosci. 2019, 10, 1603−1614

Recruited to Aggresomes in Response to Proteasome Inhibition and May Be Involved in the Ubiquitination of Hsp70-bound Misfolded Proteins. *J. Biol. Chem. 284*, 10537−10545.
(42) Waelter, S., Boeddrich, A., Lurz, R., Scherzinger, E., Lueder, G., Lehrach, H., and Wanker, E. E. (2001) Accumulation of Mutant Huntingtin Fragments in Aggresome-like Inclusion Bodies as a Result of Insufficient Protein Degradation. *Mol. Biol. Cell 12*, 1393−1407.
(43) Jana, N. R., and Nukina, N. (2003) Recent advances in understanding the pathogenesis of polyglutamine diseases: involvement of molecular chaperones and ubiquitin-proteasome pathway. *J. Chem. Neuroanat. 26*, 95−101.
(44) Jana, N. R., Tanaka, M., Wang, G., and Nukina, N. (2000) Polyglutamine length-dependent interaction of Hsp40 and Hsp70 family chaperones with truncated N-terminal huntingtin: their role in suppression of aggregation and cellular toxicity. *Hum. Mol. Genet. 9*, 2009−2018.
(45) Guzhova, I. V., Lazarev, V. F., Kaznacheeva, A. V., Ippolitova, M. V., Muronetz, V. I., Kinev, A. V., and Margulis, B. A. (2011) Novel mechanism of Hsp70 chaperone-mediated prevention of polyglutamine aggregates in a cellular model of huntington disease. *Hum. Mol. Genet. 20*, 3953−3963.
(46) Lazarev, V. F., Sverchinskyi, D. V., Ippolitova, M. V., Stepanova, A. V., Guzhova, I. V., and Margulis, B. A. (2013) Factors Affecting Aggregate Formation in Cell Models of Huntington's Disease and Amyotrophic Lateral Sclerosis. *Acta Naturae 5*, 81−89.
(47) Eenjes, E., Dragich, J. M., Kampinga, H. H., and Yamamoto, A. (2016) Distinguishing aggregate formation and aggregate clearance using cell-based assays. *J. Cell Sci. 129*, 1260.
(48) Gong, B., Lim, M. C. Y., Wanderer, J., Wyttenbach, A., and Morton, A. J. (2008) Time-lapse analysis of aggregate formation in an inducible PC12 cell model of Huntington's disease reveals time-dependent aggregate formation that transiently delays cell death. *Brain Res. Bull. 75*, 146−157.
(49) Ravikumar, B., Duden, R., and Rubinsztein, D. C. (2002) Aggregate-prone proteins with polyglutamine and polyalanine expansions are degraded by autophagy. *Hum. Mol. Genet. 11*, 1107−1117.
(50) Ramaswamy, S., McBride, J. L., and Kordower, J. H. (2007) Animal Models of Huntington's Disease. *ILAR J. 48*, 356−373.
(51) Li, J. Y., Popovic, N., and Brundin, P. (2005) The Use of the R6 Transgenic Mouse Models of Huntington's Disease in Attempts to Develop Novel Therapeutic Strategies. *NeuroRx 2*, 447−464.
(52) Marsh, J. L., Pallos, J., and Thompson, L. M. (2003) Fly models of Huntington's disease. *Hum. Mol. Genet. 12* (Spec No 2), R187−R193.
(53) Lewis, E. A., and Smith, G. A. (2016) Using Drosophila models of Huntington's disease as a translatable tool. *J. Neurosci. Methods 265*, 89−98.
(54) Steffan, J. S., Bodai, L., Pallos, J., Poelman, M., McCampbell, A., Apostol, B. L., Kazantsev, A., Schmidt, E., Zhu, Y. Z., Greenwald, M., Kurokawa, R., Housman, D. E., Jackson, G. R., Marsh, J. L., and Thompson, L. M. (2001) Histone deacetylase inhibitors arrest polyglutamine-dependent neurodegeneration in Drosophila. *Nature 413*, 739−743.
(55) Dwivedi, V., Tripathi, B. K., Mutsuddi, M., and Lakhotia, S. C. (2013) Ayurvedic Amalaki Rasayana and Rasa-Sindoor suppress neurodegeneration in fly models of Huntington's and Alzheimer's diseases. *Curr. Sci. 105*, 1711−1723.
(56) Kazemi-Esfarjani, P., and Benzer, S. (2000) Genetic suppression of polyglutamine toxicity in Drosophila. *Science (Washington, DC, U. S.) 287*, 1837−1840.
(57) Agrawal, N., Pallos, J., Slepko, N., Apostol, B. L., Bodai, L., Chang, L. W., Chiang, A. S., Thompson, L. M., and Marsh, J. L. (2005) Identification of combinatorial drug regimens for treatment of Huntington's disease using Drosophila. *Proc. Natl. Acad. Sci. U. S. A. 102*, 3777−3781.
(58) Patravale, V., Dandekar, P., and Jain, R. (2012) Nanotoxicology: evaluating toxicity potential of drug-nanoparticles. In *Nanoparticulate Drug Delivery*, pp 123−155, Woodhead Publishing.
(59) Elmore, S. A., Boyle, M. C., Boyle, M. H., Cora, M. C., Crabbs, T. A., Cummings, C. A., Gruebbel, M. M., Johnson, C. L., Malarkey, D. E., McInnes, E. F., Nolte, T., Shackelford, C. C., and Ward, J. M. (2014) Proceedings of the 2013 National Toxicology Program Satellite Symposium. *Toxicol. Pathol. 42*, 12−44.
(60) Elmore, S. A., Dixon, D., Hailey, J. R., Harada, T., Herbert, R. A., Maronpot, R. R., Nolte, T., Rehg, J. E., Rittinghausen, S., Rosol, T. J., Satoh, H., Vidal, J. D., Willard-Mack, C. L., and Creasy, D. M. (2016) Recommendations from the INHAND Apoptosis/Necrosis Working Group. *Toxicol. Pathol. 44*, 173−188.

DOI: 10.1021/acschemneuro.8b00545
ACS Chem. Neurosci. 2019, 10, 1603−1614